

---

T.V. AFANASIEVA

Taras Shevchenko National University of Kyiv  
(64/13, Volodymyrs'ka Str., Kyiv 01601, Ukraine; e-mail: Afanasieva@univ.kiev.ua)

## STUDY OF THE INTERACTION OF ATOMS OF THE IV- AND V-TH GROUPS WITH Si(001) AND Ge(001) SURFACES

PACS 82.20.Kh, 73.20.At

---

*Adsorption and diffusion processes of atoms of the IV- (Si, Ge) and V-th (As, Sb, Bi) groups on the Si(001) and Ge(001) surfaces have been simulated, by using quantum chemistry techniques. The mechanism of how the adsorption of elements of the V-th group affects the Si(001) surface is considered. The literature concerning the adsorption of atoms of the V-th group (As, Sb, Bi) and their co-adsorption with oxygen on the Si(001) surface and the diffusion of Bi ad-dimers on the Si(001) surface and Si and Ge ad-dimers on the Ge(001) one is analyzed. The results obtained demonstrate a high capability of quantum chemistry methods to provide the unique information about the interaction between adsorbates and the semiconductor surface.*

*Keywords:* adsorption, diffusion, semiconductor surface, oxidation.

### 1. Introduction

Researches aimed at elucidating how the dosed adsorption of foreign atoms affects the chemical activity of a silicon surface (as well as the surface of other semiconductors that are important from the viewpoint of their applications) is one of the challenging tasks for modern surface science and microelectronic technology. A typical example is a variation of the chemical activity of a silicon surface with respect to the oxidation after the adsorption of metal atoms. Such effects were observed at the Laboratory of Electron spectroscopy of the Taras Shevchenko National University of Kyiv headed by the Academician Mykola Grygorovych Nakhodkin. In particular, the adsorption of the atoms of elements of the V-th group (As, Sb, and Bi) on the silicon surface to a monolayer coating gives rise to the surface passivation at small oxygen exposures of about  $10^3$  L ( $1 \text{ L}(\text{langmuir}) = 10^{-6} \text{ Torr} \cdot \text{s}$ ) [1]. However, at high exposures of about  $10^6$  L for Sb [2, 3] and  $10^5$  L for Bi [4, 5], the activity of the exposed surface increases.

In the framework of another direction of researches related to the adsorption of foreign atoms to sub-monolayer quantities, the ways to create perfect Ge/Si heterostructures are intensively searched. The main obstacle consists in that Ge has a considerably larger crystal lattice constant than silicon. As a result, one cannot grow up an epitaxial film of germanium on the pure silicon surface. It turned out that some substances, e.g., As, Sb, and Bi, affect the growth conditions of a Si/Ge heterostructure, which allows an almost epitaxial coating to be obtained in a number of cases. Hence, during the Si/Ge heteroepitaxy with the participation of the atoms of elements of the V-th group (As, Sb, and Bi), complicated physico-chemical processes take place. They have to be researched in order to create the methods aimed at the controllable influence on heteroepitaxial growth, electron properties, and chemical activity and to stimulate self-assembling processes.

For the interpretation of experimental results, the computer simulation of the corresponding processes has to be carried out. The methods of quantum chemistry were selected as theoretical methods of researches.

---

© T.V. AFANASIEVA, 2015

A complication in the simulation of reactions on the Si(001) and Ge(001) surfaces consists in the necessity to consider the multiconfigurational character of wave functions for both the transition and ground states of systems. The energies of the transition states experimentally determined with an accuracy of less than 0.1 eV and a small difference between the energies of the transition states in different diffusion paths require that the methods of quantum chemistry with the maximally possible account of the electron correlation energy should be applied. However, such calculations are cumbersome and consume considerable computational resources even in the case of small clusters. On the one hand, the cluster model of a surface has to be large enough for the description of surface relaxation to be correct. On the other hand, it must contain a small number of atoms for the *ab initio* calculations to be carried out. As a result of the compromise between the level of theoretical approximations and the calculation expenses, there emerged a problem concerning the choice of adequate computation approaches.

In our works, the following methods were used: single-determinant approximations of the spin-restricted and spin-unrestricted DFT (Density Functional Theory) methods with the B3LYP (Becke 3-parameter hybrid Lee–Yang–Parr) functional, an approximation with the multireference description of wave functions CASSCF(N,M) (Complete Active Space Self-Consistent Field), and the semiempirical method MNDO-PM3 (Modified Neglect of Differential Overlap-Parametric Method 3). In order to simulate the Si(001) surface, a combined quantum mechanical–molecular mechanical (QM/MM) method with embedded clusters – SIMOMM (Surface Integrated Molecular Orbital Molecular Mechanics) – was also used. Computations were carried out with the help of software package GAMESS-US [6].

In this work, the main results of quantum chemical simulation obtained under the supervision of Academician M.G. Nakhodkin are presented. A brief analysis of literature data is also made.

## 2. Structures of Si(001) and Ge(001) Surfaces

The crystal facet Si(001) is one of the most analyzed ones in surface science. First, let us consider the structure of the (001) surface. The facet energetics governs the course of reactions on its surface

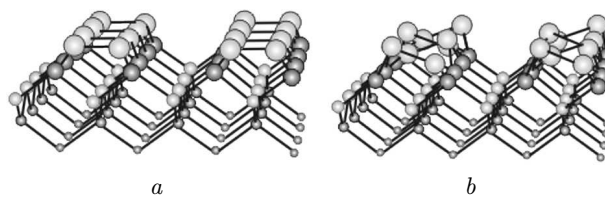


**Fig. 1.** Structures of Si(001) surfaces: (a) reconstructed Si(001) $2 \times 1$  and (b) reconstructed Si(001) $4 \times 2$

and imposes restrictions on the choice of adequate calculation models. A pure as-formed Si(001) facet is known to reconstruct itself, so that dimers are formed on the surface, which makes the number of dangling bonds half as large (Fig. 1). The dimerized Si(001) surface remains chemically active owing to the presence of dangling bonds: one per each atom in the dimer. However, the issue concerning the structure of surface dimers, namely, whether they are symmetric or buckled (asymmetric), is still under discussion. Changes in experimental conditions or the application of different theoretical methods of researches bring about different conclusions about the structure of the Si(001) surface [7–13].

Scanning tunneling microscopy (STM) researches [7] showed that, at the temperature  $T = 300$  K on the Si(001) surface, Si–Si dimers look symmetric owing to a quick “switching” between buckled (asymmetric) dimers. As the temperature decreases to 110–120 K, Si–Si dimers look buckled on STM images, because the speed of motion of Si atoms over the surface decreases [7, 8]. However, if the temperature decreases further to  $T < 40$  K, Si–Si dimers look symmetric again [8, 9]. There are some discrepancies in the explanations why the symmetric  $p(2 \times 1)$  phase appears on the Si(001) surface at low temperatures ( $T < 40$  K). In work [7], it was shown that the symmetric structure is the ground state of a surface dimer at  $T \approx 0$  K. In work [9], it was supposed that the symmetric  $p(2 \times 1)$  structure arises owing to local interaction between the dimer and the STM tip.

In theoretical researches, there are substantial discrepancies between the results of single- (DFT [10]) and multireference (MultiConfigurational Self-Consistent Field, MCSCF [11, 12]) computational methods. Buckled dimers turned out energetically favorable according to single-reference methods, and symmetric dimers according to computations taking the configuration interaction into account (Fig. 2) [11,

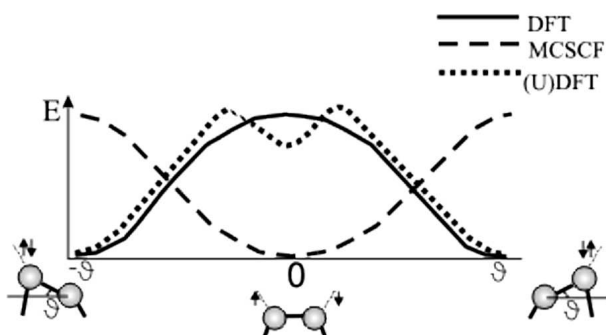


Fig. 2. Dependences of the system energy  $E$  on the buckling angle  $\vartheta$  calculated with the help of DFT and MCSCF methods

12]. According to the density functional theory, the oscillatory motion of surface silicon dimers occurs between two minima located at the buckling angles  $\vartheta \approx \pm 16^\circ$  [13]. Calculations involving the configuration interaction demonstrate an absolutely different dependence of the system energy on the buckling angle  $\vartheta$  (Fig. 2). According to MCSCF data, the surface dimer oscillates around a single minimum at  $\vartheta = 0^\circ$ . No other energy minima at  $\vartheta \neq 0^\circ$  were found [11]. The (U)B3LYP (Unrestricted B3LYP) method of the density functional theory with the broken symmetry for the systems of electrons with different spins is more suitable than the single-reference DFT/B3LYP method for constructing the wave function with regard for the multiradical character of the system. The (U)B3LYP method allowed the local minimum corresponding to the symmetric structure

Table 1. The natural orbital occupation numbers of the HOMO and LUMO for the ethylene-like  $X_2H_4$  molecules ( $X = C, Si, Ge, \text{ and } Sn$ )

X	MCSCF		MCSCF		DFT		$\vartheta$ , grad
	H	L	H	L	H	L	
	$X_2H_4$		$X(001)2 \times 1$		$X(001)4 \times 2$		
C	1.92e	0.08e	1.83e	0.17e	2e	0e	$0^\circ$ [16]
Si	1.84e	0.16e	1.71e	0.29e	2e	0e	$16^\circ$ [13]
Ge	1.82e	0.18e	–	–	2e	0e	$18^\circ$ [15]
Sn	1.78e	0.22e	–	–	2e	0e	$22^\circ$ [17]

of dimers and the global minima corresponding to the buckled geometry of dimers to be obtained [11].

The discrepancies between the computational results are explained by the fact that the DFT and MCSCF methods take different components of the electron correlation into account. The former makes allowance for the “dynamic” correlation associated with the correlated motion of electrons, whereas the quantum chemical MCSCF approximation does it for the “static” correlation that arises when the energy levels are almost degenerate.

The simplest model systems used to describe the interaction between atoms in dimers on the C(001), Si(001), Ge(001), and Sn(001) surfaces are ethylene-like molecules  $C_2H_4$ ,  $Si_2H_4$ ,  $Ge_2H_4$ , and  $Sn_2H_4$ . In ethylene-like molecules of the type  $X_2H_4$  (where  $X = C, Si, Ge, \text{ and } Sn$ ), the bond order decreases as the atomic number of  $X$  increases, because some part of the electron density becomes transferred from the highest occupied molecular orbital (HOMO) to the lowest unoccupied molecular orbital (LUMO). At the same time, the natural orbital occupation number (NOON) of the LUMO increases with the atomic number. In Table 1, the data concerning the biradical character of ethylene-like molecules are quoted [14].

The stereo surrounding of dimers C–C and Si–Si on the C (001) and Si (001) surfaces stimulates a larger transfer of the electron density from the bonding HOMO to the antibonding LUMO in comparison with planar  $C_2H_4$  and  $Si_2H_4$  molecules, as is seen from Table 1. This means that the influence of the crystal lattice enhances the biradical character of surface dimers and their activity. The more planar the structure of the dimer, the less is its biradical character, and the stronger is the dimer bond. Accordingly, the discrepancy between the results of calculations using the MCSCF or DFT methods diminishes. From Table 1, one can also see that the biradical character in ethylene-like molecules ( $C_2H_4$ ,  $Si_2H_4$ ,  $Ge_2H_4$ ,  $Sn_2H_4$ ) becomes stronger, as the atomic number increases. Therefore, we may suppose that the biradical character for the symmetric structure of surface dimers also becomes stronger, as the atomic number increases. In other words, the symmetric geometry of surface Ge dimers has a stronger biradical character in comparison with Si dimers. From Tables 1 and 2, it is evident that there can also exist a strong “static” correlation between atoms in dimers, which has to be taken into consideration, while studying the stable

Table 2. The natural orbital occupation numbers of the HOMO and LUMO in Si/Si(001), Ge/Si(001), and M/Si(001) systems ( $M = \text{As, Sb, and Bi}$ ). CASSCF(2,2)/SBK\*\* calculation method

	C/Si(001)	Si/Si(001)	Ge/Si(001)	Ge/Ge(001)	As/Si(001)	Sb/Si(001)	Bi/Si(001)
LUMO	0.02e	0.33e	0.44e	0.88e	0.02e	0.02e	0.02e
HOMO	1.98e	1.67e	1.56e	1.12e	1.98e	1.98e	1.98e

structures of dimers and ad-dimers and the elementary diffusion events of those ad-dimers. The DFT calculations [13, 15–17] show that, as the atomic number (Si, Ge, Sn) increases, the buckling angle of a surface dimer on the Si(001), Ge(001), and Sn(001) surfaces grows, and the transfer of the electron density from the lower atom in the dimer to the upper one becomes larger.

The energy difference between the symmetric and buckled structures of surface dimers on the Si(001) facet amounts to 0.1–0.2 kcal/mol [11]. The STM researches of the epitaxial growth on the Si(001) and Ge(001) surfaces [18] also testify that the energy difference between the symmetric and buckled structures of surface dimers is larger for the Ge(001) surface than for the Si(001) one. For the C(001) surface, the symmetric geometry of surface dimers was established with the help of theoretical and experimental methods [16]. Hence, theoretical and experimental data testify that the biradical structure of dimers prevails on the C(001) surface. At the same time, the biradical and zwitterionic structures compete with each other on the Si(001) surface and simultaneously coexist on the Ge(001) one.

The contributions of “dynamic” and “static” components of the electron correlation to the energy depend on the geometry of a system. This fact has a clear physical interpretation, because the buckled structure concentrates the electron density on one side of a dimer, which increases the contribution of the “dynamic” correlation. On the other hand, the “static” correlation describes the presence of degenerate states for a symmetric dimer.

The appearance of Si, Ge, As, Sb, and Bi ad-dimers on the Si(001) and Ge(001) surfaces changes the structure of their surface dimers, which become symmetric under Si, Ge, As, Sb, and Bi ad-dimers. The geometry of a surface dimer strongly depends on the geometry of neighbor surface dimers. The increase or decrease of the buckling angle of the former results

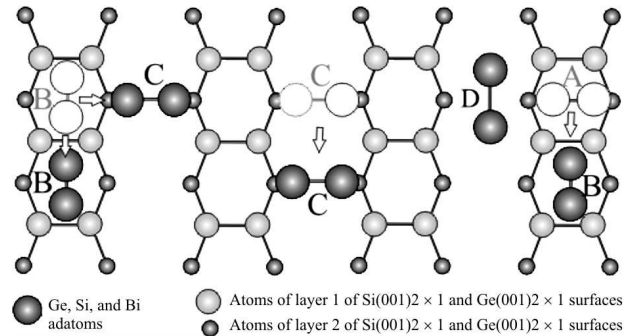
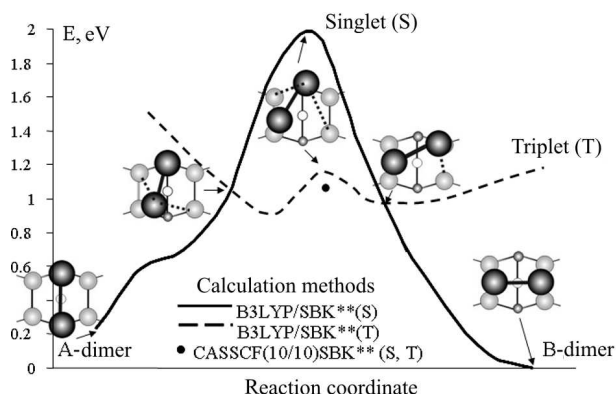


Fig. 3. Four stable adsorption sites (A, B, C, and D) for As, Sb, Bi, Ge, and Si ad-dimers on the Ge(001) and Si(001) surfaces. Elementary events of the ad-dimer diffusion on the Si(001) and Ge(001) surfaces: (B → B) of the B-type along the dimer row, (C → C) of the C-type along the dimer row; (B → C) transformation of B- into A-type, (A → B) ad-dimer rotation

in the increase or decrease, respectively, of the buckling angle of the latter. Hence, several neighbor surface dimers located along the dimer row become perturbed. The buckling angle (or the stabilization of symmetric or buckled surface dimers) can be changed by the presence of adatoms and ad-dimers, the diffusion of adatoms and ad-dimers, defects, steps, and other factors, as well as by external perturbations induced at researches, for example, the action of the STM tip. Those factors have not been studied in detail till now.

### 3. Adsorption of Si, Ge, As, Sb, and Bi Dimers on Si(001)2 × 1 Surface

Epitaxial growth researches of Si, Ge, As, Sb, and Bi films on the Si(001) surface showed that, at the initial adsorption stage of the atoms of elements of the IV-th group (Si and Ge), ad-dimers are mainly formed in the B configuration (see Fig. 3). Let us consider the electron structure of the Si(001) surface with ad-dimers (adsorbed dimers) composed of the atoms of elements of the IV- and V-th groups. In the pre-



**Fig. 4.** PES cross-sections along the most probable paths of the transformation of A-dimer Bi-Bi into B-dimer on the Si(001) surface for the singlet and triplet states of the system. The energies are reckoned from the energy of B-dimer in the singlet state in eV-units. Configurations corresponding to special points in the cross-sections of PES for singlet and triplet states are also depicted

vious section, it was shown that the electron structure of surface dimers on the Si(001) and Ge(001) surfaces can be presented as zwitterionic (buckled dimers  $X^+-X^-$ ) or biradical (symmetric dimers  $X^*-X^*$ ), where  $X = \text{Si}$  and  $\text{Ge}$ . Such systems are characterized by the presence of  $\pi$  and  $\pi^*$  states in the gap. The HOMO and the LUMO are responsible for those states. When As, Sb, and Bi dimers are adsorbed on the Si(001) surface, those states disappear, but they survive if Si and Ge dimers are adsorbed (see Table 2). From Table 2, one can see that the occupation number of the LUMO amounts to about  $0.02e$  in the M/Si(001) systems. Hence, the atoms of elements of the V-th group really saturate dangling bonds on the Si(001) surface, which governs its chemical activity. This scenario agrees with the results of experimental researches [18–23].

With the help of the STM experiment, the dimers in configurations of the A, B, and C types were observed in the Si/Si(001) system at room temperature [24–26]. Isolated Ge-Ge ad-dimers in configurations of the B and C types (sometimes in the intermediate A/B state) were observed on the Ge(001) surface [27, 28]. At the same time, only dimers in the intermediate A/B state were found in the Si/Ge(100) system [29, 30]. A question arises: Is the state A/B a new metastable configuration or a consequence of the rapid ad-dimer transformation from configuration A into configuration B? STM researches give no answer

to this question, because STM data are restricted by the rate, at which dynamic events can be distinguished.

#### 4. Diffusion of Bi Dimers on Si(001) $2 \times 1$ Surface

Experimental researches with the help of scanning tunneling microscope (STM) showed that, at first, the atoms of elements of the V-th group (Sb and Bi) are adsorbed in the form of  $\text{Sb}_4$  tetramers [31],  $\text{Bi}_4$  tetramers [32], and  $\text{Bi}_2$  dimers [33]. Under certain conditions, the atoms of elements of the V-th group (Sb and Bi) self-assemble into long ordered lines (nanolines) composed of Bi [35,36] and Sb [37] ad-dimers.

At the initial stage of the Bi adsorption on the Si(001) surface, ad-dimers are mainly formed in configurations B [34]. In the Bi/Si(001) system, very mobile and less stable ad-dimers in configurations A were found [34]. In work [34], with the help of STM, the transformation of Bi-Bi ad-dimers from configuration A into configuration B and the motion of A- and B-dimers along the dimer row were observed. According to the STM data, the diffusion activation energy for a Bi-Bi dimer in configuration B on the Si(001) surface along the dimer row amounts to 1.04 eV [34]. The activation energy of the diffusion of an A-dimer along the dimer row equals 0.82 eV [34]. The experimentally determined activation energies of rotation amount to 0.87 eV for the A-B transformation and 1.04 eV for the B-A one [34].

Calculations carried out at our laboratory using the (U)B3LYP and CASSCF methods showed that the B configuration of a Bi-Bi dimer on the Si(001) surface is the most energetically favorable one. Its energy differs from that of configuration A by 0.2 eV (Fig. 4), which is in rather satisfactory agreement with an experimental value of 0.17 eV determined with the help of STM [34]. The potential energy surface (PES) for the rotation of B-dimer Bi-Bi on the Si(001)  $2 \times 1$  surface was plotted (Fig. 4), and the optimal path for the transformation (rotation) of Bi-Bi ad-dimer from configuration A into B ( $A \rightarrow B$ ) was found. This path corresponds to such a correlated motion of Bi adatoms, when they move one-by-one. The energy barrier of the  $B \rightarrow A$  transformation equals 1.1 eV, which agrees with a magnitude of 1.04 eV obtained experimentally with the help of STM [34]. An important achievement is the account that the system has

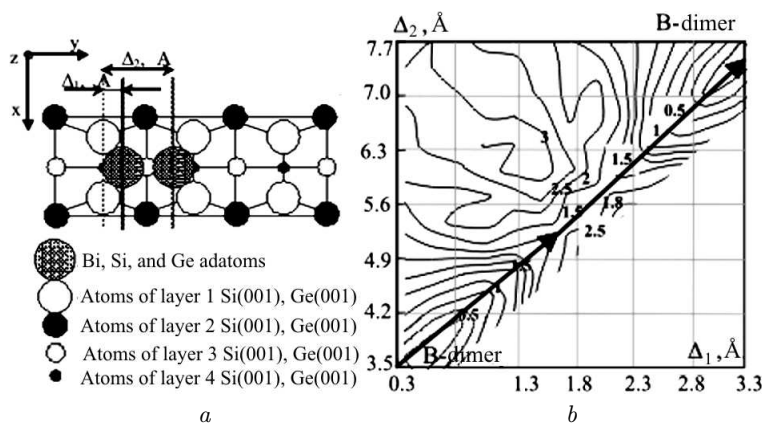


**Fig. 5.** (a) Displacements of ad-dimer atoms ( $\Delta_1$  and  $\Delta_2$ ) along the dimer row. (b) PES and the diffusion path of B-dimer Bi–Bi along the dimer row on the Si(001) $2 \times 1$  surface. The PES is presented in the form of a map of equipotential curves. Numbers near the equipotential curves mean the adsorption energies of ad-dimers at the corresponding point reckoned in eV-units from the energy of B-dimer

a 100%-biradical character in the transition state of its path. Such a one-by-one motion of Bi atoms at the rotation turned out more energetically favorable than the simultaneous motion of Bi atoms proposed in the literature. In the latter case, the activation energy of the B  $\rightarrow$  A transformation was considered to equal 1.48 eV [38].

In work [39], the PES for the diffusion of B-dimer Bi–Bi along the dimer row on the Si(001) $2 \times 1$  surface was built (Fig. 5). The activation barrier in this case was found to equal 1.79 eV (Fig. 6). At transition state TS, the system has a multiradical character. The most probable path of the diffusion of B-dimer Bi–Bi is the motion of the intact ad-dimer without dissociation along the dimer row on the Si(001) $2 \times 1$  surface.

### 5. Diffusion of Si and Ge Dimers on Ge(001) $2 \times 1$ Surface

STM researches showed that the dynamics of separate adatoms on the surface is very complicated. Separate adatoms move rapidly even at a temperature of 160 K. At room temperature, those adatoms form ad-dimers characterized by rather high diffusion and dissociation barriers, so that they avoid the formation of large structures. Ad-dimers Si–Si, Ge–Ge, and Si–Ge can move and rotate on the Si(001) and Ge(001) surfaces (Fig. 3) [24–30].

In Table 3, experimental and calculated values for the rotation and diffusion barriers of Si, Ge, and

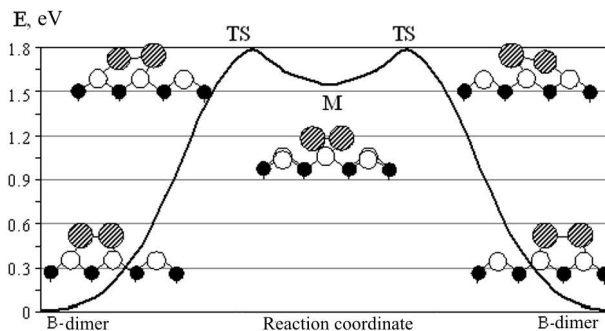


**Fig. 6.** Dependence of the adsorption energy on the diffusion path and the main atomic configurations acquired during the motion along the diffusion path calculated with the use of the CASSCF(8,8)/SBK\*\* method. Configurations TS correspond to transition states, and configuration M to the local minimum

**Table 3.** Diffusion barriers for B-dimers Si–Si and Ge–Ge on the Si(001) and Ge(001) surfaces. The STM results measured at room temperature are shown in parentheses. The energy barriers are presented in eVs

	Ge/Ge(001)	Si/Ge(001)	Ge/Si(001)	Si/Si(001)
A $\rightarrow$ B	0.3 [51]	0.4 [50, 51]	(0.82 [40]) 0.74 [45]	(0.68 [24]) (0.65 [42]) (0.82 [48])
B $\rightarrow$ B	0.95 [47, 49] (0.82 [47])	0.9 [47, 49] (0.83 [47])	(1.01 [41]) (0.77 [46])	0.94 [43] 1.09 [44] (0.94 [42]) 1.02 [44]

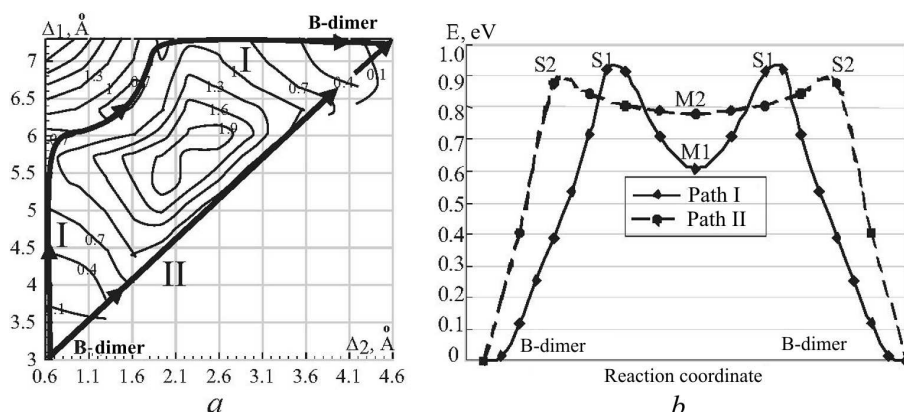


**Fig. 7.** (a) PES and (b) the most probable paths (I and II) of the diffusion of B-dimer Ge–Ge along the dimer row on the Ge(001) surface calculated using the (U)B3LYP/N21-3\*\* method. Numbers near the equipotential curves mean the adsorption energies of ad-dimers at the corresponding point reckoned in eV-units from the energy of B-dimer

Bi ad-dimers on the Si(001) and Ge(001) surfaces are quoted. One can see that the diffusion of ad-dimers on the Si(001) surface is more anisotropic than that on the Ge(001) one. The fastest is the diffusion of B-dimers along the dimer rows [24–30]. However, a number of questions arise: How do ad-dimers move on the surface? Are the atoms in a diffusing ad-dimer bound with each other? Or do they diffuse independently and afterward form a dimer again?

Despite that the adsorption of Si and Ge dimers on the Si(001) surface has been intensively studied recently, there exists a certain discrepancy between the results obtained. In work [46], it was shown that, when B-dimers Si (Ge) diffuse along a dimer row on the Si(001) surface, Si (Ge) adatoms move correlatively, i.e. one-by-one. In the course of such a motion, the dimer bond breaks. The diffusion along the path, when the dimer bond does not break, and the dimer moves as a whole, was found to be less energetically favorable. In work [41], another path of the diffusion of B-dimer was proposed, when the ad-dimer moves as a whole and rotates.

Our computations using the (U)B3LYP method showed that the energy barriers for the Si–Si and Ge–Ge ad-dimers on the Ge(001) surface to rotate from the epitaxial configuration (B-dimer) to the non-epitaxial one (A-dimer) amount to about 0.3 and 0.4 eV, respectively [51]. Adatoms in the Si–Si and Ge–Ge ad-dimers move one-by-one, when ad-dimers rotate, similarly to the motion of Bi adatoms at the

A→B transformation (Fig. 4). A small value of energy barrier indicates that the A/B minimum experimentally revealed with the use of STM is a result of the quick rotation of Si–Si and Ge–Ge ad-dimers on the Ge(001) surface.

The diffusion of Ge–Ge, Si–Si, and Bi–Bi ad-dimers on the Ge(001) and Si(001) surfaces has similar diffusion properties. The motion of atoms forming the Ge–Ge, Si–Si, and Bi–Bi ad-dimers is correlated at the rotation: first, one adatom moves, whereas the other remains motionless; then, the second atom starts to move (Fig. 4).

We also built the PESs for the diffusion of B-dimers Ge–Ge (Fig. 7, a) and Si–Si on top of a dimer row on the Ge(001) surface [47, 49]. The dependences of the adsorption energy along the optimal diffusion paths of B-dimer Ge–Ge are shown in Fig. 7, b. The dependences of the adsorption energy of Si–Si ad-dimer along paths I and II have almost the same form. The corresponding atomic configurations for paths I and II are shown in Fig. 8. Path I corresponds to the correlation motion of adatoms, when, first, one of the adatoms (upper) moves into the neighbor cell, and the other remains in the initial state; then, the second adatom follows the first one and forms a dimer with it in the neighbor cell (Fig. 8). Path II corresponds to the motion of the entire non-dissociated ad-dimer along the dimer row.

The barrier height for the diffusion of germanium and silicon B-dimers along the dimer row on the Ge(001) surface amounts to about 0.9 and 0.95 eV, re-

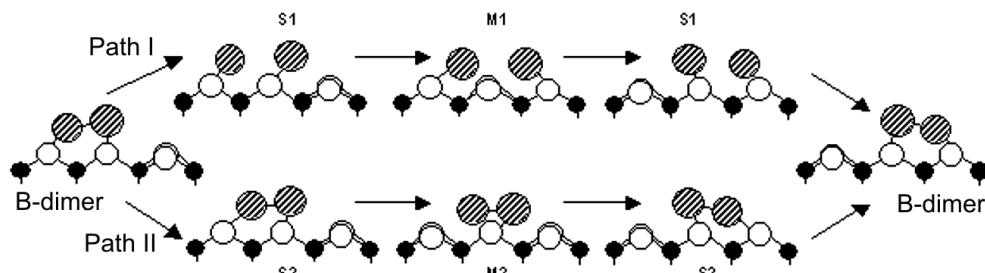


**Fig. 8.** Main atomic configurations during the motion along paths I and II. Configurations S1 and S2 correspond to transition states, and configurations M1 and M2 to local minima

spectively [47, 49]. Those values agree well with magnitudes of 0.82 and 0.83 eV obtained with the help of STM [47].

### 6. Electric Field Effect on the Dynamics of Si–Si and Si–Ge Ad-dimers on Si(001) Surface

In works [24, 41, 45, 48], the influence of an electric field on the rotation ( $A \rightarrow B$ ) of Si–Si ad-dimer and its diffusion along the dimer row ( $B \rightarrow B$ ) on the Si(001) surface was analyzed. The applied electric field was found to reduce the activation energy barrier both at positive and negative potential differences. In works [45, 46], paths for the rotation of Si–Si, Si–Ge, and Ge–Ge ad-dimers on the Si(001) surface were proposed. The rotation activation energies calculated for Si–Si and Ge–Si ad-dimers agree with experimental values (see Table 3). However, the calculated dependences of the corresponding transition state energies on the applied electric field strength do not correspond to experimental ones [41, 48]. In works [41, 48], another path of the diffusion of B-dimer along the dimer row on the Si(001) surface was proposed, which includes the rotation and the translation of Si–Si and Si–Ge ad-dimers. The energy barriers corresponding to those paths also agree with experimental data, but, unlike work [46], the dependences of the energy barriers on the applied electric field strength also agree with the experiment. A comparison between the calculated and experimentally obtained dependences of the barriers for elementary diffusion events (rotation  $B \rightarrow A$  and diffusion  $B \rightarrow B$ ) on the electric field applied perpendicularly helps us to determine the most probable path of diffusion. This circumstance is important when different diffusion mechanisms have close values of activation barriers.

The transition state of the reaction has a higher polarizability than stable configurations owing to the

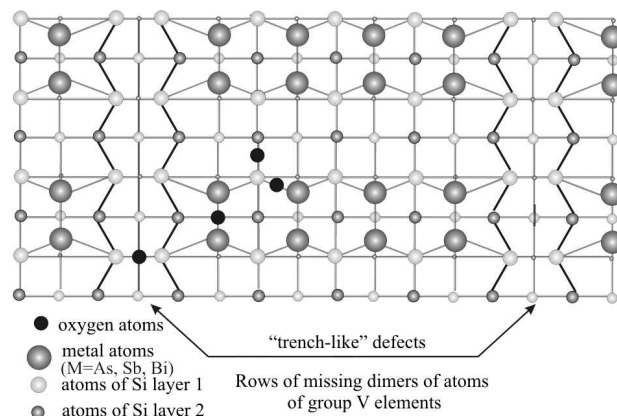


**Fig. 9.** Model of  $M/\text{Si}(001)-2 \times 5$  surface ( $M = \text{As}, \text{Sb}, \text{and Bi}$ ). Places of atomic oxygen adsorption are shown

presence of dangling bonds. In work [52], it was shown that the electric field changes the electron density distribution, which complicates the comparison of experimental data with the results of calculations carried out for the zero field. Transition states, in which some bonds break and other ones rebond, most often require that multireference wave functions, which allow a partial population of MO and adequately describe degenerate and pseudodegenerate states, should be used in calculations. In work [52], it was shown that, in systems with partially filled MOs, variations in the electron and geometrical structures under the action of an external electric field are considerable.

### 7. Formation of Monolayer Coatings from the Atoms of Elements of the V-th Group (As, Sb, and Bi) on Si(001) Surface

Experimental data [19–23] testify that the atoms of elements of the V-th group (As, Sb, and Bi) passivate the  $\text{Si}(001)2 \times 1$  surface by saturating silicon surface dangling bonds at coating thicknesses close to

1 ML (monolayer). According to experimental data, a  $(2 \times n)$ -superstructure, where  $n$  depends on the temperature, is formed in the Sb/Si(001) and Bi/Si(001) systems [20,54]. This structure consists of  $n-1$  dimers with a missing Bi(Sb) dimer and forms a vacancy-line or trench-like defect, as is shown in Fig. 9. The formed M/Si(001)- $2 \times n$  surface structure, as well as the M/Si(001)- $2 \times 1$  one, has no dangling bonds [20, 54]. The formation of  $(2 \times n)$ -superstructures is a result of the surface stress anisotropy, which increases with the atomic number for the As, Sb, and Bi monolayer coatings. The surfaces As/Si(001)-1ML, Sb/Si(001)-1ML, and Bi/Si(001)-1ML have the identical dimer structure  $(2 \times 1)$ , but the electron structures of their metal-silicon interfaces are different. In works [22, 55], it was shown that the system Sb/Si(001) demonstrates core-level energy shifts of surface silicon atoms than the system As/Si(001) does. We have analyzed the transfer of the electron density between the adsorbate and the substrate in all three systems [49]. The minimum charge  $Q = +0.13e$  is transferred in the Sb/Si(001) system. The charge transferred in the As/Si(001) system is larger ( $Q = +0.19e$ ), and this value coincides with the literature data [51, 52]. At last, the charge transferred in the Bi/Si(001) system is maximum ( $Q = +0.37e$ ). There is a relation between the electron density transfer and the core-level energy shifts. As a rule, the larger the atomic charge, the stronger is the energy shift of internal levels. We also calculated the  $2p$  core-level shifts of surface silicon atoms [57]. The Si core-level shifts in the Sb/Si(001) system turned out minimum, and in the Bi/Si(001) one maximum. Earlier, it was demonstrated [55] that the chemical energy shift of silicon core levels observed in the Sb/Si(001) system is smaller than that in the As/Si(001) one, which may possibly be connected with the fact that lower stresses develop in the former system. In all three systems, the metal atoms accumulate a positive charge, but, owing to the influence of the lone pair of  $s$ -electrons in the metal, the dipole moment changes differently in different systems. Hence, the work function should also vary. Those conclusions require an additional experimental verification. This is the more so because the work function and other electron parameters of the semiconductor near-surface region are highly important for understanding the mechanism of its work in various semiconductor devices.

## 8. Interaction of Oxygen with As/Si(001), Sb/Si(001), and Bi/Si(001) Surfaces

The results of calculations using the B3LYP and MNDO-PM3 methods testify that atomic oxygen adsorbed on the M/Si(001)-1 ML surface forms M-O-M, M-O-Si, and Si-O-Si bridge structures [53]. The latter are the most probable for defect-free M/Si(001)-1 ML surfaces. It was shown that, in the presence of trench-type defects formed by missing metal dimers, Si-O-Si bridges are formed first between silicon atoms in the upper silicon layer; afterward, Si-O-Si bridges are formed under the upper layer of silicon atoms with shallower extremes of the adsorption energy. The shifts of  $3d$  and  $4d$  core levels of As and Sb atoms, respectively, were determined [57]. The shifts of  $3d$  core levels of As agree with the literature data [1, 55, 56]. In work [53], it was proved that atomic oxygen becomes really formed the Si-O-Si, Si-O-M, and M-O-M bridge structures.

The dissociation of an oxygen molecule adsorbed on the M/Si(001)-1 ML surface at trench-type defects or at surface double vacancies of the atoms of metals of the V-th group was simulated using the MNDO-PM3 methods [53]. The existence of both activation and nonactivation processes at the dissociation of an oxygen molecule was demonstrated. A reduction of the energy barrier, as the atomic number of adatoms belonging to elements of the V-th group grows, is typical of activation processes [53, 58].

## 9. Conclusions

A successfully selected collection of adequate methods for the analysis of available models, or models proposed by us, and the application of complex computational clusters allow the influence of the electron correlation to be taken into account and the new reliable data concerning elementary events of ad-dimer diffusion on the surfaces of atomic semiconductors in the Bi/Si(001), Ge/Ge(001), and Si/Ge(001) systems to be obtained. The barrier heights for elementary diffusion events of B-dimers Ge and Si on the Ge(001) surface and B-dimers Bi on the Si(001) one were determined with the help of high-level quantum chemical computations. B-dimers Bi were shown to diffuse on the Si(001) surface following a complicated scenario, when the system dwells in states with partial populations of bonding and antibonding orbitals. The

correspondence between theoretically and experimentally obtained values of diffusion barriers testify to the adequacy of the model proposed for the description of elementary diffusion events.

A new model was proposed for the interaction between oxygen adatoms and the M/Si(001) surfaces, where M is a metal atom of the V-th group. In this model, atomic oxygen, being adsorbed on the M/Si(001)-1 ML surface, forms M–O–M, M–O–Si, and Si–O–Si bridge structures. The most probable for defect-free M/Si(001)-1 ML surfaces is the Si–O–Si bridge structures.

1. F. Rochet, C. Poncey, G. Dufour *et al.*, Surf. Sci. **326**, 229 (1995).
2. I.P. Koval, Yu.A. Len and M.G. Nakhodkin, Nanosyst. Nanomater. Nanotekhnol. **3**, 941 (2005).
3. I.P. Koval, V.V. Laposha, Yu.A. Len *et al.*, Visn. Kyiv. Univ. Ser. Fiz. Mat. Nauky, N 4, 307 (2002).
4. I. Koval, P. Melnik, N. Nakhodkin *et al.*, Surf. Sci. **384**, L844 (1997).
5. M.Yu. Pyatnitskii, I.F. Koval', P.V. Mel'nik *et al.*, Teor. Eksp. Khim. **33**, 124 (1997).
6. M.W. Schmidt, K.K. Baldrige, J.A. Boatz *et al.*, J. Comput. Chem. **14**, 1347 (1993).
7. R.A. Wolkow, Phys. Rev. Lett. **68**, 2636 (1992).
8. Y. Kondo, T. Amakusa, M. Iwatsuki *et al.*, Surf. Sci. **453**, L318 (2000).
9. K. Hata, S. Yoshida, and H. Shigekawa, Phys. Rev. Lett. **89**, 286104 (2002).
10. S.B. Healy, C. Filippi, P. Kratzer *et al.*, Phys. Rev. Lett. **87**, 016105 (2001).
11. Y. Jung, Y. Shao, M.S. Gordon *et al.*, J. Chem. Phys. **119**, 10917 (2003).
12. R.M. Olson and M.S. Gordon, J. Chem. Phys. **124**, 081105 (2006).
13. S.J. Jenkins and G.P. Srivastava, J. Phys. Condens. Matter **8**, 6641 (1996).
14. M.S. Gordon, M.W. Schmidt, G.M. Chaban *et al.*, Chem. Phys. **110**, 4199 (1999).
15. S.C.A. Gay and G.P. Srivastava, Phys. Rev. B **60**, 1488 (1999).
16. H. Tamura and M.S. Gordon, J. Chem. Phys. **119**, 10318 (2003).
17. H.M. Tutuncu, G.P. Srivastava, and T.T. Guzelsoy, Surf. Sci. **566–568**, 900 (2004).
18. P. Kruger and J. Pollmann, Phys. Rev. Lett. **74**, 1155 (1995).
19. K. Sakamoto, K. Kyoya, K. Miki *et al.*, Jpn. J. Appl. Phys. **32**, L204 (1993).
20. A.G. Mark, J.A. Lipton-Duffin, J.M. MacLeod *et al.*, J. Phys. Condens. Matter. **17**, 571 (2005).
21. I.F. Koval, P.V. Melnik, N.G. Nakhodkin *et al.*, Surf. Sci. **331–333**, 585 (1995).
22. M.Yu. Pyatnitskii, I.F. Koval', P.V. Mel'nik *et al.*, Teor. Eksp. Khim. **32** 168 (1996).
23. D.H. Rich, F.M. Leibsle, A. Samsavar *et al.*, Phys. Rev. B **39**, 12758 (1989).
24. B.S. Swartzentruber, A.P. Smith, and H. Jonsson, Phys. Rev. Lett. **77**, 2518 (1996).
25. H.J.W. Zandvliet, B. Poelsema, and B.S. Swartzentruber, Phys. Today **54**, 40 (2001).
26. Z. Zhang, F. Wu, H.J.W. Zandvliet *et al.*, Phys. Rev. Lett. **74**, 3644 (1995).
27. H.J.W. Zandvliet, T.M. Galea, E. Zoethout *et al.*, Phys. Rev. Lett. **84**, 1523 (2000).
28. T.M. Galea, C. Ordas, E. Zoethout *et al.*, Phys. Rev. B **62**, 7206 (2000).
29. W. Wulfhekel, B.J. Hattink, H.J.W. Zandvliet *et al.*, Phys. Rev. Lett. **79**, 2494 (1997).
30. E. Zoethout, H.J.W. Zandvliet, W. Wulfhekel *et al.*, Phys. Rev. B **58**, 16167 (1998).
31. Y.W. Mo, Science **261**, 886 (1993).
32. M. Naitoh, M. Takei, S. Nishigaki *et al.*, Surf. Sci. **482–485**, 1440 (2001).
33. S.Yu. Bulavenko, I.F. Koval, P.V. Melnik *et al.*, Surf. Sci. **507–510**, 119 (2002).
34. S.Yu. Bulavenko, I.F. Koval, P.V. Melnik *et al.*, Surf. Sci. **482–485**, 370 (2001).
35. M. Naitoh, H. Shimaya, S. Nishigaki *et al.*, Appl. Surf. Sci. **142**, 38 (1999).
36. J.H.G. Owen, K. Miki, and D.R. Bowler, J. Mater. Sci. **41**, 4568 (2006).
37. S. Rogge, R.H. Timmerman, P.M.L.O. Scholte *et al.*, Phys. Rev. B **62**, 15341 (2000).
38. K. Chuasiripattana and G.P. Srivastava, Phys. Rev. B **71**, 153312 (2005).
39. T. Afanasieva, I. Koval, M. Nakhodkin, in *Proceed. of the Int. Sci. Conference "Physical and Chemical Principles of Formation and Modification of Micro- and Nanostructures" (FMMN'2008), Kharkiv, Ukraine, 8–10 October 2008*, Vol. 2, p. 471.
40. X.R. Qin and B.S. Swartzentruber, Phys. Rev. Lett. **842**, 4645 (2000).
41. L.M. Sanders, R. Stumpf, T.R. Mattsson *et al.*, Phys. Rev. Lett. **91**, 206104 (2003).
42. C.C. Fu, M. Weissmann, and A. Saul, Surf. Sci. **481**, 97 (2001).
43. B.S. Swartzentruber, Phys. Rev. Lett. **76**, 459 (1996).
44. B. Borovsky, M. Krueger, and E. Ganz, Phys. Rev. Lett. **78**, 4229 (1997).
45. Z.Y. Lu, F. Liu, C.Z. Wang *et al.*, Phys. Rev. Lett. **85**, 5603 (2000).
46. Z.Y. Lu, C.Z. Wang, and K.M. Ho, Phys. Rev. B **62**, 8104 (2000).

47. T.V. Afanasieva, S.Yu. Bulavenko, I.F. Koval *et al.*, *J. Appl. Phys.* **93**, 1452 (2003).
48. T.R. Mattsson, B.S. Swartzentruber, R. Stumpf *et al.*, *Surf. Sci.* **536**, 121 (2003).
49. T. Afanasieva, I. Koval, M. Nakhodkin, *Visn. Kyiv. Univ. Ser. Fiz. Mat. Nauky*, N 1, 207 (2007).
50. T.V. Afanasieva, I.F. Koval, N.G. Nakhodkin *et al.*, *Surf. Sci.* **482-485**, 702 (2001).
51. T. Afanasieva, I. Koval, M. Nakhodkin, in *Proceed. of the Int. Sci. Conference "Physical and Chemical Principles of Formation and Modification of Micro- and Nanostructures" (FMMN'2010), Kharkiv, Ukraine, 6-8 October 2010*, Vol. 2, p. 484.
52. T.V. Afanasieva, A.A. Greenchuck, I.P. Koval *et al.*, *Ukr. Fiz. Zh.* **56**, 240 (2011).
53. T.V. Afanasieva, I.F. Koval, and N.G. Nakhodkin, *Surf. Sci.* **507-510C**, 788 (2002).
54. T. Hanada and M. Kawai, *Surf. Sci.* **242**, 137 (1991).
55. J.K. Cho, M.H. Kang, K. Terakura, *Phys. Rev. B* **55**, 15464 (1997).
56. G. Li and Y.C. Chang, *Phys. Rev. B* **50**, 8675 (1994).
57. T.V. Afanasieva, I.F. Koval, Yu.A. Len *et al.*, *Ukr. Fiz. Zh.* **50**, 685 (2005).
58. T.V. Afanasieva, V.O. Glavadski, I.F. Koval *et al.*, *Ukr. Fiz. Zh.* **46**, 1280 (2001).

Received 22.09.14.

Translated from Ukrainian by O.I. Voitenko

*Т.В. Афанас'єва*

ДОСЛІДЖЕННЯ ВЗАЄМОДІЇ  
АТОМІВ ЕЛЕМЕНТІВ IV ТА V ГРУП  
З ГРАНЯМИ Si(001), Ge(001)

Р е з ю м е

Наведено результати досліджень адсорбції та дифузії атомів елементів IV (Si, Ge), V (As, Sb, Bi) груп на поверхні Si(001) та Ge(001) методами квантової хімії. Досліджено механізм впливу адсорбції атомів елементів V групи на властивості грані (001) кремнію. Проаналізовано роботи, присвячені проблемам адсорбції та коадсорбції атомів елементів V групи (As, Sb та Bi) та кисню на поверхні Si(001), дифузії аддимерів Bi на поверхні Si(001) та аддимерів Si, Ge на поверхні Ge(001). Результати досліджень демонструють високий потенціал методів квантової хімії для отримання унікальної інформації про взаємодію адсорбатів з поверхнею напівпровідника.